2 Kinetic models in protein folding

OLIVER BIERI and THOMAS KIEFHABER

1. Introduction

Experimental work on the mechanism of protein folding has been greatly influenced by Levinthal's famous paper of 1969 (1), in which he pointed out that a polypeptide chain would require an astronomical time to explore at random all possible conformations in order to finally reach the native state. This motivated the search for partially folded intermediates guiding the protein to the native state. Although many proteins have been found to fold through transient intermediates (for reviews see refs 2–10), more recent theoretical studies have sparked off a discussion on their role in the folding process. Simplified models for polypeptide chains, in combination with energy landscape theory, suggested that the Levinthal paradox could be resolved by a small energy bias against locally unfavourable conformations (11). This would reduce folding rates to the experimentally observed timescales. As a common representation of the theoretical work, funnel-like folding landscapes were proposed (12–19) in which the polypeptide chain has a vast number of different possible ways of reaching the native state. Partially folded states observed in these models mainly represent misfolded states trapped in local energy minima rather than obligatory folding intermediates. It is suggested that the polypeptide chain does not encounter major energy barriers for the actual folding process and that the rate of folding is limited by a region in the folding funnel where the gain in energy cannot compensate for the loss in conformational entropy (14, 15). Thus, the folding kinetics are proposed to be determined mainly by entropic barriers.

In this chapter we shall first present an overview of the experimental results from kinetic studies on protein folding and unfolding reactions over the past 30 years. By analogy to the treatment of simple chemical reactions, the existence was assumed of well-defined pathways involving a limited number of kinetic species. In combination with transition-state theory, these studies aimed at detecting and characterizing intermediates and the transition states in the folding process. In the second part of the chapter we shall treat alternative reaction-rate theories, which may provide more realistic descriptions of protein-folding reactions, and we shall see how the experimental data can be interpreted in terms of such models.

2. Analysis of protein-folding reactions using simple kinetic models

In studies of reaction kinetics the aim is to try to find the minimal model capable of describing the experimental data. It is thereby assumed that the mechanism involves a finite number of kinetic species which are separated by energy barriers significantly larger than the thermal energy ($>5k_BT$), but each kinetic species may consist of different conformations in rapid equilibrium. This allows the transitions between two species (X_i and X_j) to be described with microscopic rate constants for the forward (k_{ij}) and reverse (k_{ji}) reactions:

$$X_i \underset{k_{ji}}{\overset{k_{ij}}{\rightleftharpoons}} X_j \qquad [1]$$

2.1 General treatment of kinetic data

Experimental studies on the mechanism of protein folding focused mainly on monomeric proteins as model systems. This has the major advantage that all observed reactions are of the first order. As a consequence, the time-dependent change in intensity (P) of an observed signal can be represented as a sum of n exponentials with relaxation times τ_i ($=1/\lambda_i$) and corresponding amplitudes (A_i)

$$P_t - P_\infty = \sum_{i=1}^{n} A_i \cdot e^{-\lambda_i t} \qquad [2]$$

where P_t is the observed intensity at time t, and P_∞ is the intensity at $t \rightarrow \infty$. The apparent rate constants, λ_i, are generally functions of all microscopic rate constants, k which depend on external parameters such as temperature, pressure, and denaturant concentration. The amplitudes, A_i, depend additionally on the initial concentrations of the kinetic species. There is a general relationship between the number of apparent rate constants and the number of kinetic species, n. Any kinetic mechanism with n different species connected by first-order reactions results in $n - 1$ observable rate constants. Applied to protein folding with fixed initial (U) and final (N) states, the observation of $n - 1$ apparent rate constants thus indicates the presence of $n - 2$ transiently populated intermediate states (a more detailed treatment of the analysis of kinetic data in protein folding is given in ref. 20 and general overviews are described in 21 and 22).

2.2 Kinetics of two-state folding

Experimental investigations have revealed simple two-state folding without detectable intermediates for more than 20 small proteins (for an overview see ref. 23):

$$U \underset{k_u}{\overset{k_f}{\rightleftharpoons}} N \qquad [3]$$

where k_f and k_u are the microscopic rate constants for the folding and unfolding reactions, respectively. The single observable macroscopic rate constant (λ) for this mechanism is readily derived as:

$$\lambda = k_f + k_u. \quad [4]$$

The equilibrium of the reaction is determined by the flows from the native state N to the unfolded state U and vice versa:

$$k_f [U]_{eq} = k_u [N]_{eq} \quad [5]$$

and the equilibrium constant (K) for folding is

$$K = \frac{[N]_{eq}}{[U]_{eq}} = \frac{k_f}{k_u}. \quad [6]$$

The most striking (and straightforward) parameter to be inferred from two-state behaviour is the free energy for folding ($\Delta G°$) which is connected by the van't Hoff relation with the equilibrium constant (K):

$$\Delta G° = -RT \ln K = -RT \ln\left(\frac{[N]_{eq}}{[U]_{eq}}\right) = -RT \ln\left(\frac{k_f}{k_u}\right). \quad [7]$$

Thus the stability can be measured in two different ways, either by equilibrium methods or by kinetic measurements. It is worth noting that, in the case of a protein that follows two-state folding behaviour, the free energies for folding inferred from the two methods have to agree.

2.3 Transition-state analysis for two-state folding

The commonly applied analysis of two-state folding is based mainly on concepts from transition-state theory (TST). TST connects a rate constant, k, to the free energy of activation ($\Delta G°‡$) for forming the transition or activated state (‡). which is assumed to be the point of highest free energy along the reaction coordinate (24)

$$k = \kappa \frac{k_B T}{h} e^{-\frac{\Delta G°‡}{RT}}. \quad [8a]$$

k_B is the Boltzmann constant, h the Planck constant, and κ is a transmission factor with an upper limit of 1. The absolute value of ($\Delta G°‡$) depends strongly on the correct pre-exponential factor, which reflects the maximum rate of the reaction in the absence of free-energy barriers. This problem will be discussed in the second part of the chapter (see also Chapter 5). To simplify the treatment of kinetic data, the conventional transition-state theory (CTST) is used, in which κ is assumed to be 1, given by

$$k = \frac{k_B T}{h} e^{-\frac{\Delta G°‡}{RT}}. \quad [8b]$$

Experimental analyses of kinetic and equilibrium folding data have revealed linear

free-energy relationships between $\Delta G_f^{\circ\ddagger}$, $\Delta G_u^{\circ\ddagger}$, ΔG°, and the concentration [D] of a chemical denaturant such as urea or guanidinium chloride (4, 25–27).

$$\begin{aligned} \Delta G_u^{\circ\ddagger}(\mathrm{D}) &= \Delta G_u^{\circ\ddagger}(\mathrm{H_2O}) + m_u^{\ddagger}[\mathrm{D}] \\ \Delta G_f^{\circ\ddagger}(\mathrm{D}) &= \Delta G_f^{\circ\ddagger}(\mathrm{H_2O}) + m_f^{\ddagger}[\mathrm{D}] \\ \Delta G^\circ(\mathrm{D}) &= \Delta G^\circ(\mathrm{H_2O}) + m[\mathrm{D}] \end{aligned} \qquad [9]$$

where (H_2O) denotes the values in the absence of denaturant and (D) those at a given denaturant concentration [D]. Thus, according to eqns 4, 8a, and 9, a plot of lnλ versus denaturant concentration yields a V-shaped curve for two-state folders (a chevron plot, Fig. 1), which allows k_f and k_u to be determined over the entire range of denaturant concentration. Substituting eqn 8b in eqn 6, using eqn 9, yields

$$\Delta G^\circ(\mathrm{H_2O}) = \Delta G_f^{\circ\ddagger}(\mathrm{H_2O}) + \Delta G_u^{\circ\ddagger}(\mathrm{H_2O}) \qquad [10]$$

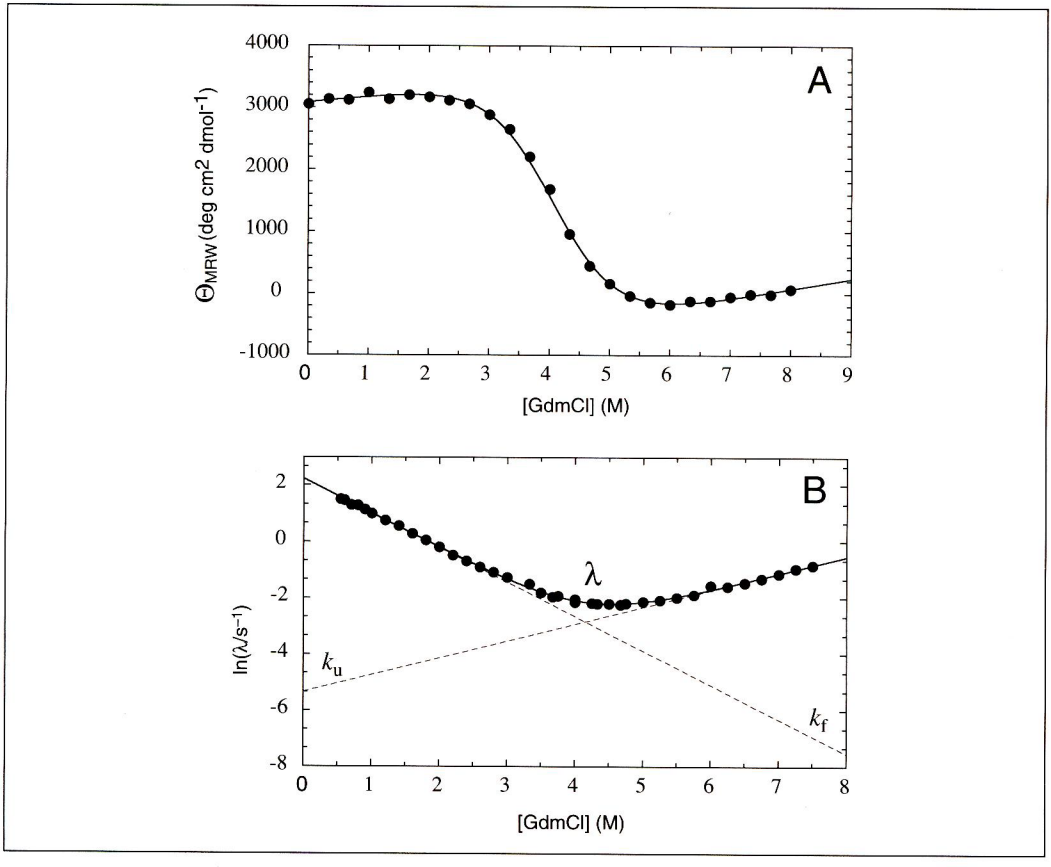

Fig. 1. (A) GdmCl-induced unfolding transition of tendamistat at pH 2 and (B) the GdmCl dependence of the apparent rate constant (λ) under the same conditions. The GdmCl-dependence of lnλ is dominated by lnk_f below 3 M GdmCl and by lnk_u above 6 M GdmCl. The solid line represents a fit of the data according to eqns 4, 8 and 9. This yields lnk_f and lnk_u over the complete range of GdmCl concentrations (- - - -). (Pappenberger and Kiefhaber, unpublished results.)

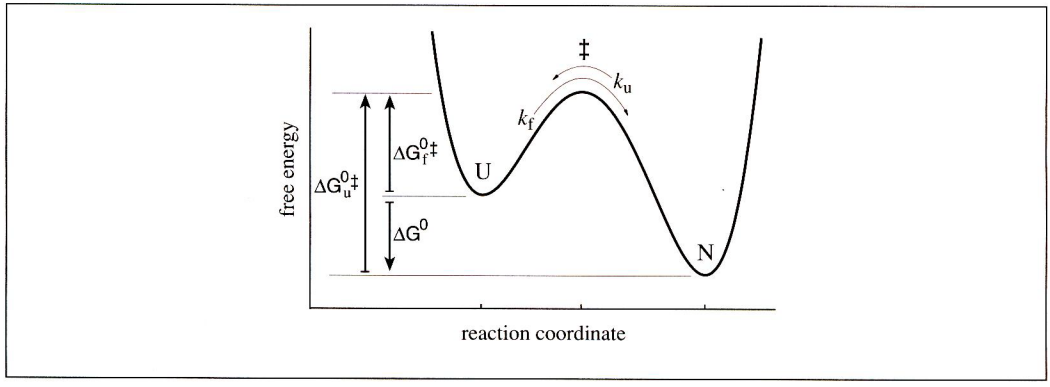

Fig. 2. The relationships between the free energies of activation for folding, $\Delta G_f^{\circ‡}$, and unfolding, $\Delta G_u^{\circ‡}$, and of the equilibrium free energy, ΔG°, using conventional transition-state theory.

and

$$m = m_f^‡ - m_u^‡. \qquad [11]$$

The relationship between ΔG°, $\Delta G_f^{\circ‡}$, and $\Delta G_u^{\circ‡}$, is shown in Fig. 2.

3. Characterization of the transition states in protein folding

Transition-state theory allows the use of classical concepts from physical chemistry to characterize the rate-limiting steps in protein-folding reactions. The Gibbs fundamental equation of chemical thermodynamics:

$$dG = Vdp - SdT + \sum_i \mu_i dn_i \qquad [12]$$

can be adapted to protein-folding transitions, including the effect of a chemical denaturant, D, on protein stability:

$$\Delta G^\circ = \Delta V^\circ dp - \Delta S^\circ dT + m d[D]. \qquad [13]$$

Using CTST and eqn 13 yields the free energies of activation for the folding and unfolding reactions

$$\Delta G^{\circ‡} = \Delta V^{\circ‡} dp - \Delta S^{\circ‡} dT + m^‡ d[D]. \qquad [14]$$

Thus, $\Delta V^{\circ‡}$, $\Delta S^{\circ‡}$, and $m^‡$ can be obtained by varying the pressure, the temperature, or the denaturant concentration, respectively.

3.1 Denaturant dependence of folding kinetics

The equilibrium m-value is found to correlate with the difference in solvent-accessible surface area (SASA) between the native and unfolded protein (4, 26). By analogy the kinetic m-values, $m_f^‡$ and $m_u^‡$ are thought to reflect changes in SASA between the un-

folded and transition states and the native and transition states, respectively (4). Comparison of the value of $m_f^{\ddagger}$ for the folding reaction with the equilibrium value m can thus be used to draw conclusions about the degree of organization $\alpha(= m_f^{\ddagger}/m)$ of the transition state. Kuwajima and co-workers characterized the transition state of folding of α-lactalbumin and apo-α-lactalbumin and concluded that the structural organization of the activated state in this protein is about 65% native-like in respect of its exposure to GdmCl (28). For most two-state folders, α-values lie between 0.6 and 0.9, indicating a rather compact and native-like transition state.

3.2 Temperature dependence of folding kinetics

Pohl (29) was the first to apply the Eyring formalism to the temperature dependence of protein folding and unfolding kinetics. From eqn 14 we see that the change in $\Delta G^{\circ\ddagger}$ with temperature (at constant pressure and GdmCl concentration) corresponds to $\Delta S^{\circ\ddagger}$. We can use eqn 8b to apply this relation to the temperature dependence of rate constants. Since the pre-exponential factor in CTST contains the temperature (eqn 8b), it is more convenient to divide the rate constant by the temperature T and use the equation:

$$\frac{k}{T} = \frac{k_B}{h} e^{-\Delta G^{\circ\ddagger}/RT} = \frac{k_B}{h} e^{\Delta S^{\circ\ddagger}/R} \cdot e^{-\Delta H^{\circ\ddagger}/RT}. \qquad [15]$$

Studies on several proteins, including chymotrypsin (29), chymotrypsin inhibitor CI2 (30), cold-shock protein (31), tendamistat (32), and protein L (33), have shown that $\Delta H^{\circ\ddagger}$ and $\Delta S^{\circ\ddagger}$ are temperature dependent, indicating that $\Delta c_p^{\ddagger} \neq 0$. Thus the relationships

$$\Delta H^{\circ\ddagger}(T) = \Delta H^{\circ\ddagger}(T_o) + \Delta C_p^{\ddagger} \cdot (T + T_o) \qquad [16]$$

$$\Delta S^{\circ\ddagger}(T) = \Delta S^{\circ\ddagger}(T_o) + \Delta C_p^{\ddagger} \cdot \ln(T/T_o) \qquad [17]$$

where T represents a given temperature and T_o an arbitrary reference temperature, commonly 25 °C, are used to rewrite eqn 15 as:

$$\ln\frac{k}{T} = \ln\frac{k_B}{h} - \frac{1}{RT}\left[\Delta H^{\circ\ddagger}(T_o) - T\Delta S^{\circ\ddagger}(T_o) + \Delta C_p^{\ddagger} \cdot (T - T_o - T\ln\frac{T}{T_o})\right]. \qquad [18]$$

Consequently, a plot of $\ln(k/T)$ against $1/T$ (Eyring plot) yields $\Delta C_p^{\ddagger}$, $\Delta H^{\circ\ddagger}$, and $\Delta S^{\circ\ddagger}$ (Fig. 3). The observed temperature effects for protein-folding reactions match the temperature dependence of hydrophobic interactions (34, 35), indicating that water could play a crucial role in the rate-limiting steps.

3.3 Pressure dependence of folding kinetics

In protein folding, formation of the native state is usually accompanied by an increase in volume, which has contributions from volume changes associated with

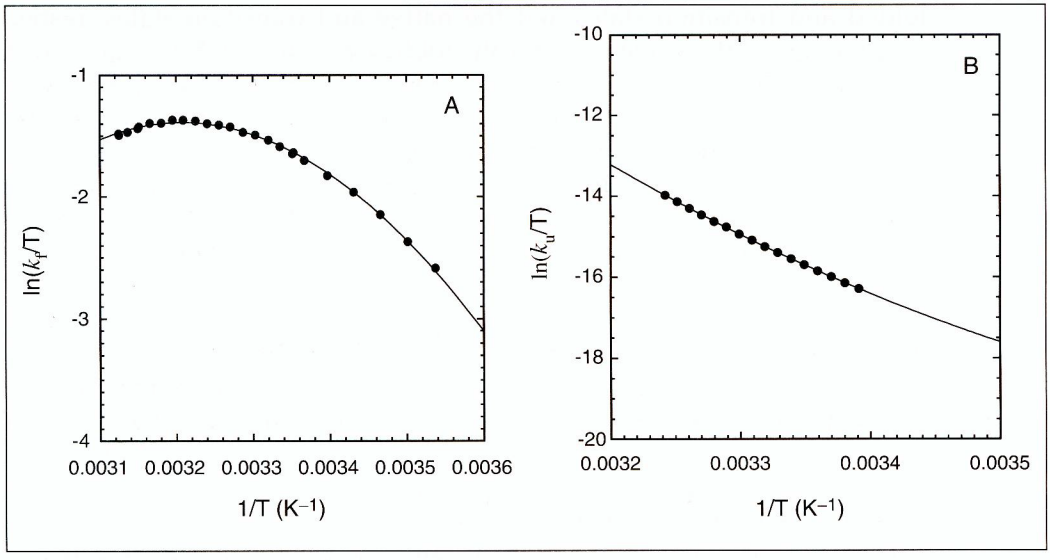

Fig. 3. Eyring plots of the temperature dependence of the microscopic rate constants for (A) the refolding (k_f), and (B) the unfolding (k_u) reactions of tendamistat. Both plots show a pronounced curvature indicating a finite $\Delta C_p^{\ddagger}$ for both reactions. Analysis of the data by applying eqn 18 at T_o = 298.15 K yields for refolding a $\Delta H^{o\ddagger}$ of 6.68 ± 0.06 kcal/mol, a $T\Delta S^{o\ddagger}$ of –8.36 ± 0.06 kcal/mol and a $\Delta C_p^{\ddagger}$ of –0.49 ± 0.01 kcal/(molK), and for unfolding a $\Delta H^{o\ddagger}$ of 28.80 ± 1.49 kcal/mol, a $T\Delta S^{o\ddagger}$ of 5.36 ± 1.40 kcal/mol and a $\Delta C_p^{\ddagger}$ of 0.60 ± 0.03 kcal/(molK). Data are taken from ref. 77.

released water molecules (36–38) and with the atoms of the polypeptide chain (39, 40) on forming a solvent-inaccessible core. In addition, packing deficiencies in the native state add to the observed effects (41). The pressure dependence of folding and unfolding rates can therefore give valuable information on the structure and the hydration properties of the transition state. Planck (42) was the first to note that the pressure dependence of a chemical equilibrium reflects the difference in volume between the initial and final states. From eqn 14 we can relate the pressure dependence of $\Delta G^{o\ddagger}$ to the activation volume, $\Delta V^{o\ddagger}$, i.e. the volume change between the initial state of a reaction and the transition state. At constant temperature and denaturant concentration:

$$\left.\frac{\partial \Delta G^{o\ddagger}}{\partial p}\right|_{T,[D]} = -\Delta V^{o\ddagger}. \qquad [19]$$

Using CTST (eqn 8), this is equivalent to:

$$\left.\frac{\partial \ln k}{\partial p}\right|_{T,[D]} = -\frac{\Delta V^{o\ddagger}}{RT}. \qquad [20]$$

Thus $\Delta V^{o\ddagger}$ can be determined by measuring the pressure dependence of the microscopic rate constants for folding and unfolding.

Volume changes in protein folding are commonly around 20–100 cm^3/mol for small monomeric proteins (36), which represents 1–2% of the total protein volume. Pressure-jump experiments on the refolding and unfolding kinetics of several proteins have revealed that the volume of the transition state is commonly native-like (43, 44). The volume profile of the folding of tendamistat was investigated with high-pressure stopped-flow experiments over a broad range of GdmCl concentrations. The results showed strong and compensating effects of the denaturant on the activation volumes for both refolding and the unfolding reactions (45). As a consequence, the reaction volume remains constant over the accessible range of GdmCl concentrations, but the volume of the transition state becomes increasingly native-like with increasing denaturant concentrations. Above 5 M GdmCl the volume of the transition state even exceeds the volume of the native state, arguing for a solvent-shielded transition state with packing deficiencies under these conditions.

4. Complex folding kinetics

For simple, two-state folding reactions the microscopic rate constants are readily obtained from the chevron plot (Fig. 1) and the reactions can be analysed using transition-state theory. However, for most proteins, folding is more complex and non-linear chevron plots are observed. These non-linearities can have different origins. The transient population of partially folded intermediates frequently occurs under native-like solvent conditions, i.e. at low denaturant concentrations. This will lead to a change in the folding mechanism and thus to a change in the slope of $\ln\lambda$ versus denaturant concentration, concomitant with the appearance of additional kinetic phases (46) (see Section 4.2). Nevertheless, a change in the folding mechanism can also occur without transiently populated intermediates (see Section 4.5). Kinetic coupling between two-state folding and slow equilibration processes in the unfolded state provides a third source for non-linear chevron plots (47) (Section 4.1). Since these possible origins for complex folding kinetics have far-reaching effects on the molecular interpretation of the kinetic data, it is crucial to be able to discriminate between them.

4.1 Heterogeneity in the unfolded state

The unfolded state of a protein consists of a large ensemble of different conformations which are in rapid equilibrium, and can thus be treated as a single kinetic species as long as their interconversion is faster than the kinetic reactions leading to the native state. On the other hand, slow interconversion reactions between the different unfolded conformations lead to kinetic heterogeneity. This was first observed by Garel and Baldwin (48), who showed that both fast- and slow-refolding molecules exist in unfolded ribonuclease A (RNase A). This was interpreted in terms of *cis–trans* isomerization of Xaa–Pro peptide bonds by Brandts and co-workers in 1975 (49), a proposal that has been confirmed for several proteins (50–52). Whenever folding and proline isomerization have similar rates, or when folding is slower than isomerization, a pronounced curvature is observed in the refolding limb of the chevron plot,

which looks similar to the effect of transiently populated intermediates (20, 47). The effect of prolyl isomerization on folding kinetics and its identification as a rate-limiting step is discussed in detail in Chapter 8. The effect on chevron plots is treated quantitatively in ref. 47.

Another cause of kinetic heterogeneity in the unfolded state was identified in cytochrome *c*, where parallel pathways were shown to be due to the exchange of the haem ligands in the unfolded state (53–55) (see Chapter 3).

4.2 Transiently populated intermediates

Multi-exponential kinetics are observed when partially folded states accumulate transiently during the folding process. As discussed above, the number of kinetic species, n, is related to the number, $n-1$, of observable rate constants and, with unfolded and native state as the initial and final states, the number of intermediates is given by $n-2$. Thus, for a single observable rate constant there are no intermediates, corresponding to two-state folding. The observation of two apparent rate constants indicates a single intermediate, etc. It should be noted that these considerations only apply if there is a kinetically homogeneous unfolded state with rapidly interconverting conformations. In the case of heterogeneous populations of unfolded molecules, the number of observable rate constants is additionally correlated with the number of unfolded species.

The first step, therefore, in elucidating a folding mechanism should be the determination of the number of exponentials needed to describe the data. To this end, kinetics are usually monitored using a number of different probes. In addition, it is crucial to look for burst-phase reactions, i.e. for processes occurring within the experimental deadtime. These reactions are observed for many proteins during refolding and are caused by a considerable compaction of the polypeptide chain (56) (see Chapters 3 and 5). Whether rapid collapse represents a distinct step on a folding pathway, or whether it is the response of the unfolded state to the change in solvent conditions upon refolding, is currently under investigation. Results on the folding of α-lactalbumin (57, 58) and apomyoglobin (59) suggest that there is at least some cooperativity in burst-phase intermediates with a limited number of specific interactions.

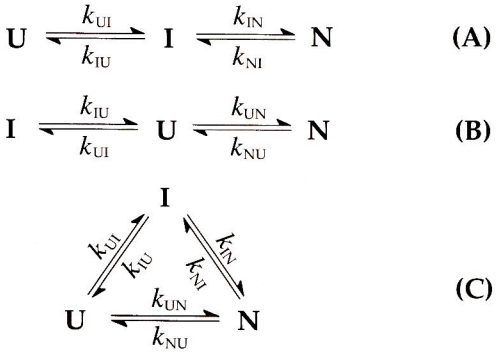

[Scheme 1]

The next step is to locate the intermediates in the folding process. In the simplest case, with a single intermediate, two apparent rate constants will be observed for all possible three-state mechanisms, independently of the number of microscopic rate constants (Scheme 1). The analysis for mechanisms A and B simplifies when equilibration between U and I occurs on a much faster time scale than folding to the native state (60, 61). Formation of the intermediate can then be treated as a rapid pre-equilibrium. The apparent rate constants for mechanism A (on-pathway intermediate) can thus be approximated by:

$$\lambda_1 = k_{UI} + k_{IU} \quad \text{and} \quad \lambda_2 = \frac{1}{1 + 1/K_{UI}} \cdot k_{IN} + k_{NI} \quad \text{with} \quad K_{UI} = \frac{k_{UI}}{k'_{IU}} \qquad [21]$$

and for mechanism B (off-pathway intermediate) as:

$$\lambda_1 = k_{UI} + k_{IU} \quad \text{and} \quad \lambda_2 = \left(1 - \frac{1}{1 + 1/K_{UI}}\right) \cdot k_{IN} + k_{NI} \qquad [22]$$

where $1/(1+ (1/K_{UI}))$ represents the fraction of intermediate (f(I)) in the pre-equilibrium. Since I is productive in mechanism A and non-productive in mechanism B, the rate of formation of N depends on f(I) and $1-f$(I), respectively. Due to the commonly observed strong denaturant dependencies of the microscopic rate constants, the simplifications made above might not be valid in a certain range of denaturant concentrations. Therefore, the simplified treatment of the data should only be performed if formation of the intermediate is too fast to be measured. In all other cases, the exact solutions of the three-state model should be used to fit the data. These solutions are available from most kinetic textbooks. A particularly useful source for the analytical solution of a vast number of different kinetic mechanisms is the excellent article by Szabo (21).

Under conditions where the simplifications in eqns 20 and 21 hold, they provide a tool for identifying off-pathway intermediates. Destabilization of the intermediate leads to a larger fraction of productive (unfolded) molecules in the off-pathway model. Thus, addition of denaturant will speed up folding when the resulting destabilization of the intermediate exceeds the deceleration of the N $\rightarrow$U reaction. As a consequence, an increase in the folding rate with increasing concentrations of denaturant points to the transient accumulation of an off-pathway intermediate. This behaviour has been observed for intermediates trapped by non-native disulphide bonds (62), by non-native proline isomers (63), and by non-specific aggregation (64).

4.3 A case study: the mechanism of folding of lysozyme

To illustrate the need for rigorous treatment of the kinetic data in order to determine the folding mechanism we shall discuss the folding of hen egg-white lysozyme. Lysozyme consists of two structural subdomains, the α-domain with exclusively α-helical structure and the β-domain with predominantly β-structure (65, 66). Starting from GdmCl-unfolded, disulphide-intact protein, large changes in far-UV CD and fluorescence signals are observed within the first millisecond of refolding (67–70).

Time-resolved small-angle X-ray scattering experiments show that this burst-phase reaction leads to a globular state, with a significantly smaller radius of gyration (R_g) than the unfolded protein (56). In a subsequent reaction, with a time constant of 30 ms (at pH 5.2 and 20°C), a well-defined intermediate state is formed, as observed by strong quenching in tryptophan fluorescence to a level below that of the native state (56, 70), by a decrease in the far-UV ellipticity (67–69), and by a further compaction of the polypeptide chain (56). Pulsed hydrogen/deuterium-exchange experiments show that this intermediate has native-like helical structure in the α-domain whereas the β-sheet structures are not formed (69). The intermediate converts to the native state with a relaxation time of about 400 ms. There have been controversial reports as to the role of this intermediate in the folding process (69, 70) and it remained unclear whether it is an obligatory intermediate on the folding pathway for all lysozyme molecules.

The observation of two apparent rate constants (treating the burst phase, rapid collapse as a pre-equilibrium uncoupled from the slower reactions) cannot rule out any of the mechanisms shown in Scheme 1. However, comparing mechanism A with mechanisms B and C offers a simple means of distinguishing obligatory from non-obligatory folding intermediates. In the case of an obligatory intermediate, all folding molecules have to fold through this state, resulting in a lag phase in the formation of native molecules. However, direct spectroscopic measurements, or measurements of changes in R_g are not able to monitor formation of native lysozyme directly, since changes in spectroscopic and geometric properties usually occur in all folding steps. In addition, the use of inhibitor binding to detect the formation of active lysozyme did not give any clear-cut results, since binding is too slow under the applied experimental conditions (70, 71). An experimental approach to determining the amount of native molecules and of folding intermediates at any point during a refolding reaction was described by Schmid and first applied to distinguish between parallel and sequential pathways in the prolyl isomerization-limited folding of RNase A (72). These experiments consist of two consecutive mixing steps. In a first step, refolding is initiated from completely unfolded protein. The folding reaction is allowed to proceed for a certain time (t) and then the solution is transferred to a high concentration of denaturant. This results in the unfolding of all native molecules and of partially folded states which have accumulated in the refolding step. Each state (N or I) is characterized by a specific unfolding rate constant at high concentrations of denaturant, where unfolding is virtually irreversible, so that little kinetic coupling occurs. The amplitudes of the observed unfolding reactions consequently reflect the amounts of the respective species present at time (t) when refolding was interrupted. Thus, varying the time (t) allowed for refolding gives the time course of the populations of native lysozyme and of the intermediate during the folding process.

In the folding of lysozyme, two unfolding reactions are observed in interrupted refolding experiments (71, 73). One of them corresponds to the well-characterized unfolding reaction of native lysozyme, and a second, much faster one corresponds to unfolding of the intermediate. The collapsed state unfolds too fast under all conditions to be measured by stopped-flow mixing. The results show that the inter-

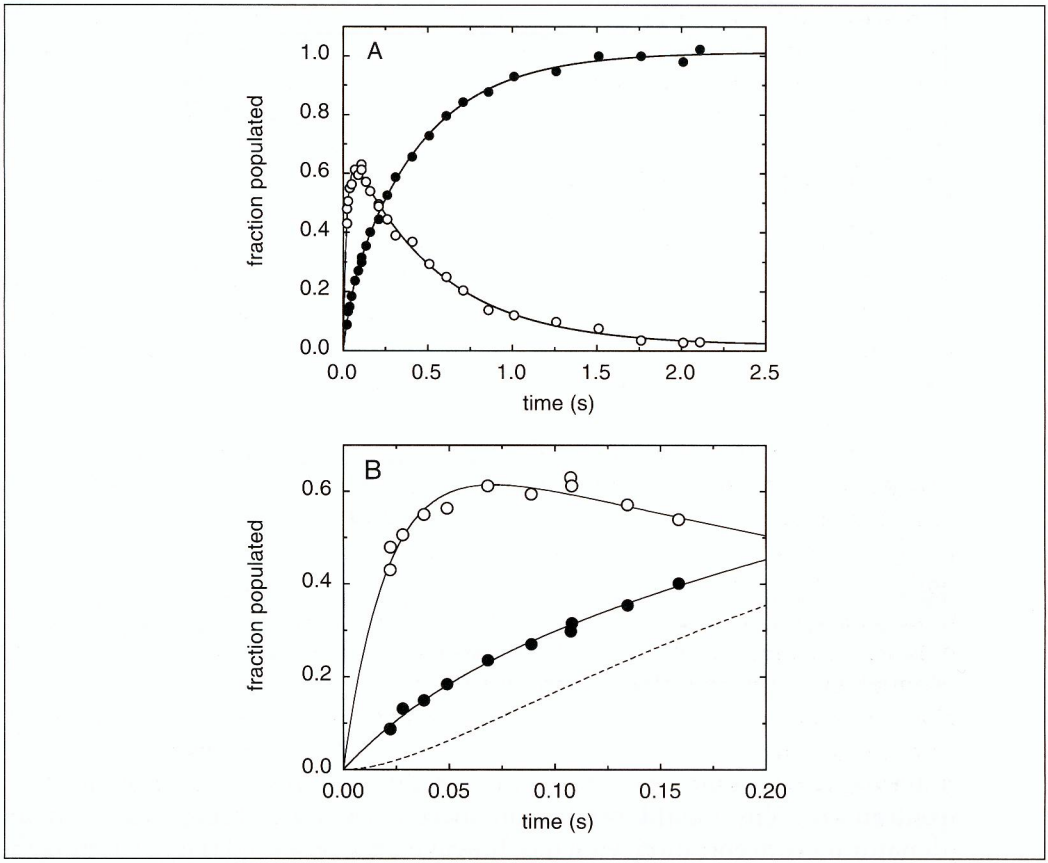

Fig. 4. (A) Time course of formation of native molecules (●) and of a folding intermediate (○) during the folding of lysozyme. (B) The early time region of the kinetics shows that the faster process (τ = 30 ms) produces both native molecules and the partially folded intermediate. The lag expected for a linear on-pathway mechanism (----) is not observed. Data are taken from refs 71 and 73.

mediate is not obligatory for lysozyme folding, since no lag phase in forming native lysozyme is observed (Fig. 4). Rather, formation of I and formation of 20% of the native molecules both occur with the faster kinetic phase (τ = 30 ms). The slower process (τ = 400 ms) reflects the interconversion of the intermediate to the native state, resulting in the remaining 80% of the molecules folding to the native state (71). As discussed above, identical apparent rate constants for forming the intermediate and native molecules on a fast pathway are expected, since any three-state model gives rise to only two observable rate constants.

These results rule out a linear on-pathway three-state model (mechanism A in scheme 1), but they cannot distinguish between mechanisms B and C. Performing a least-squares fit of the denaturant-dependence of the two apparent rate constants to the analytical solutions of both models revealed that only the triangular model was able to describe the data (73). In the case of the off-pathway model, unfolding of the

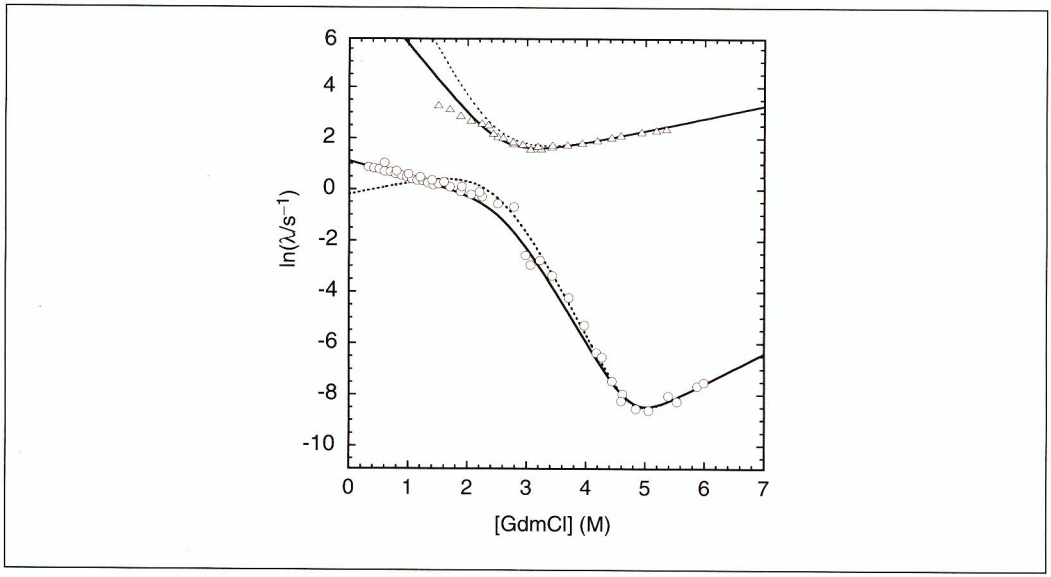

Fig. 5. GdmCl-dependence of the two apparent rate-constants for lysozyme folding (○, △) and least-squares fits to the analytical solutions of the triangular model (—; Scheme 1, mechanism C) and to the linear off-pathway model (.....; Scheme 1, mechanism B). The fits show that the off-pathway model is not able to describe the data at low GdmCl concentrations. Data are taken from ref. 73.

intermediate becomes the rate-limiting step for folding at very low denaturant concentrations. This would predict an increase in the folding rate with increasing denaturant concentration, which is, however, not observed (Fig. 5). Fitting the data to the circular three-state model allowed all six microscopic rate-constants to be determined (Fig. 6). These rate constants can be analysed using CTST to yield the relative free energies of the three kinetic species and of the transition states connecting them (73).

This case study demonstrates the need for methods capable of detecting the time course of individual kinetic species during the folding process. Direct spectroscopic measurements will, in most cases, not be able to provide this information. In addition, the folding of lysozyme shows that for complex reactions it is usually impossible to assign experimentally observed rate constants directly to individual steps on folding pathways, since they are complex functions of several microscopic rate constants. In order to determine the microscopic rate constants it is essential to elucidate the folding mechanism, which is facilitated by the use of interrupted refolding assays to specifically monitor the time course of individual kinetic species. This method can also be applied to more complex folding mechanisms with more than one intermediate (74).

On the practical level, it should be noted that it is essential to plot the data on a linear time scale when looking for lag phases, since even simple exponential kinetics show a sigmoidal time course on a logarithmic time scale.

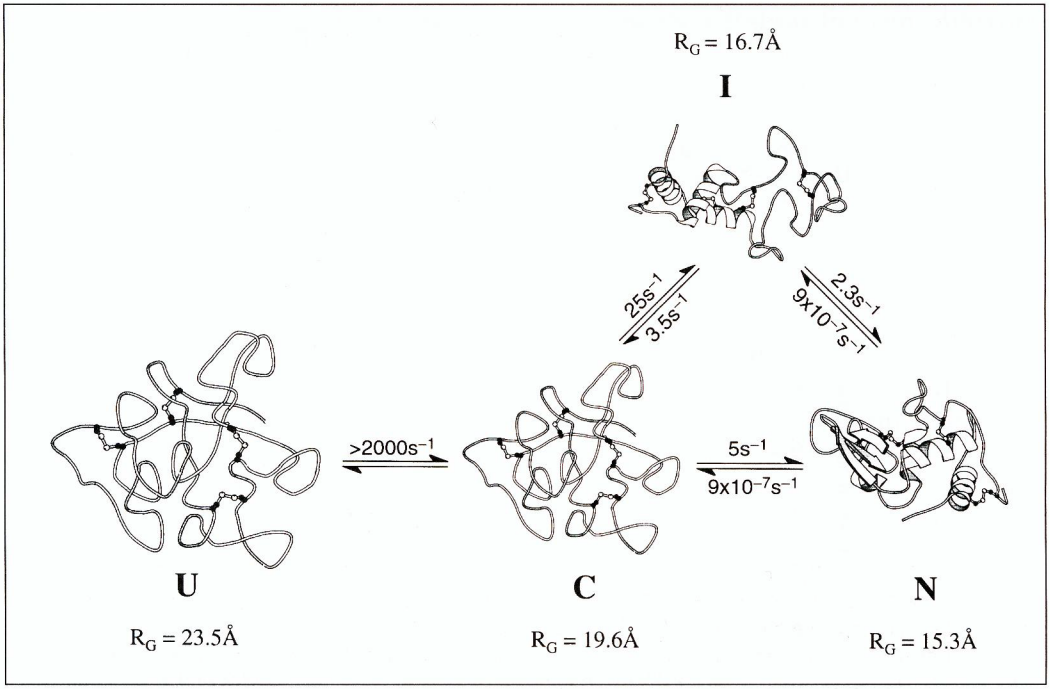

Fig. 6. Folding mechanism of lysozyme obtained by combining a large number of experimental data, using the various methods described in refs 69, 71, 73, and 56.

4.4 Significance of small differences in rates observed with different probes

Small differences in the rate constants are often observed when the folding process is monitored by different probes, such as fluorescence and far-UV CD. It has been argued that this might indicate consecutive steps on a linear pathway or parallel pathways for formation of secondary and tertiary structure. As discussed above, the apparent rate constants in protein-folding reactions are usually complex functions of all microscopic rate constants and thus do not generally reflect individual folding steps. To demonstrate this, we simulated folding kinetics involving two intermediates with very different spectroscopic parameters, located either on a sequential or a parallel pathway. We assumed that one signal, e.g. fluorescence, changes completely in forming one intermediate (I_1) with no change for the other signal, e.g. far-UV CD. Formation of a second intermediate (I_2) occurs with a slightly different rate constant and is accompanied by signal changes in the far-UV CD, but not in fluorescence. We then simulated the observed time course of both intermediates and the resulting changes in fluorescence and CD for the consecutive (Fig. 7A–C) and parallel pathways (Fig. 7D–E). As expected, the simulations show three apparent rate constants for both four-state mechanisms. The consecutive mechanism (Fig. 7A) shows a significant lag phase in formation of the second intermediate (I_2), also observed if folding is

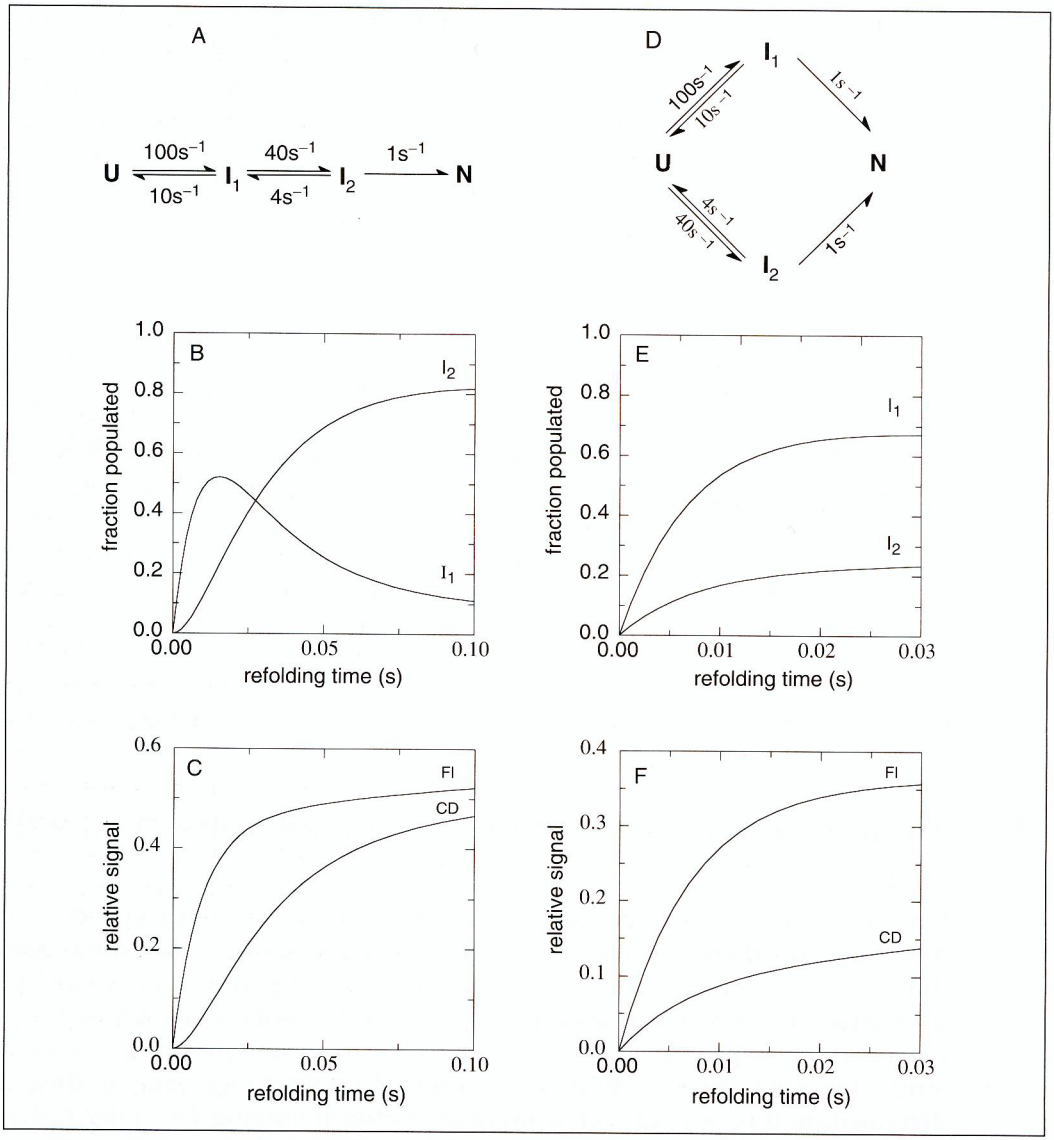

Fig. 7. Simulation of a sequential mechanism (A–C) and of a parallel mechanism (D–F) for folding involving two intermediates with very different CD and fluorescence properties. Panels B and E display the early regions of the time course of the two intermediates. Panels C and F show the corresponding fluorescence and CD changes, assuming the spectroscopic properties described in the text.

monitored by far-UV CD (Figs 7B and C). In the case of parallel pathways, both intermediates are formed in the fastest reaction, which has a larger rate constant than any of the microscopic rate constants, due to kinetic coupling (Fig. 7E). The intermediates are, however, formed to different extents, reflecting the differences in the microscopic rate constants for their formation. This is to be expected for competing

reactions (22). Thus, CD and fluorescence measurements will show the same rate constants but different amplitudes (Fig. 7F). These simulations demonstrate that caution has to be taken in assigning apparent rate constants to individual folding steps and argue against the significance of small differences in rate constants monitored by different probes. Such differences in most cases reflect errors, often caused by slightly different conditions in different experiments.

4.5 Complex transition barriers

For simple two-state systems $\ln k_u$ and $\ln k_f$ typically show linear dependencies on the denaturant concentration. In some cases, however, non-linearity in the denaturant dependence of $\ln k_u$ has been observed in the absence of populated intermediates and without contributions from prolyl isomerization reactions (75–81). For these proteins the slope of $\ln k_u$ versus [D] decreases with increasing denaturant concentration. Two explanations have been offered for this behaviour. The curvature in the chevron plots of spliceosomal protein U1A (81) and CI2 (80) was interpreted in terms of Hammond behaviour, which has been observed for several reactions in organic chemistry (82). Hammond behaviour states that the transition state of a reaction moves structurally towards that state to which it moves closer in energy. In terms of protein folding, destabilization of the native state with increasing concentrations of denaturant (45, 80) or by mutation (83) will result in the movement of the transition state to a more native-like structure. This can explain the decrease in slope of $\ln k_u$ with increasing denaturant concentration. An alternative interpretation of the same results is to suggest a rough transition-state barrier containing a large number of local minima (80, 84) corresponding to high-energy intermediates. Similar barriers have been observed in theoretical studies (85, 86) and shown to accelerate protein folding due to a favourable entropic contribution to the free energy of activation (87). The transitions between the various intermediates are assumed to be denaturant dependent, leading to a change in the rate-limiting transition with varying denaturant concentration. This model is supported by results on the unfolding of various proteins, which show a clear kink rather than a rollover in the chevron plot (76, 77, 79). This behaviour can be explained by the presence of a single, non-populated, high-energy intermediate in the transition barrier.

In addition to local minima in the barrier, many theoretical models have predicted a large number of parallel pathways giving rise to a multidimensional barrier region. For n parallel pathways a single apparent rate constant, λ, which is the sum of the forward and reverse rate constants, will be observed for all pathways, as long as no intermediates are populated:

$$\lambda = \sum_{i=1}^{n} (k_{f_i} + k_{u_i}). \qquad [23]$$

As a consequence, two-state folding will still be observed and the complexity cannot be detected experimentally.

5. Folding without barriers

Theoretical models have been proposed in which the actual folding reaction is an energetically downhill process limited only by entropic barriers (15). Zwanzig treated protein folding as a rapid, barrier-less equilibration reaction between many unfolded conformations linked to a barrier-less escape process, which can only take place from a limited number of unfolded conformations or 'escape states' (88), similar to the flow out of a bath tub. Simulation of the dynamic behaviour of such a system shows that single exponential kinetics result when the transitions between the different unfolded states are fast and the number of escape states is small compared to the total number of unfolded conformations. This process can thus not be distinguished experimentally from two-state folding kinetics with an energy barrier. A more general treatment of the effect of entropy barriers on chemical dynamics shows that single exponential kinetics are always observed (at least for reactions in solution) in the absence of energetic (enthalpic) barriers, as long as entropic barriers exist (89). These considerations highlight the difficulties in discriminating between different folding models on the basis of single exponential behaviour, since the same experimentally observed kinetics can result from considerably different folding landscapes.

6. Non-exponential kinetics

Non-exponential kinetics were first reported by Kohlrausch (90) for the relaxation of glass fibres after stretching. He described a broad distribution of relaxation times covering timescales of several orders of magnitude. Such non-exponential kinetics can be treated with a stretched exponential term of the kind:

$$A = A_0 \, e^{-(k\,t)^{\beta}}. \qquad [24]$$

The stretch factor β indicates a time-dependent change in the rate constant k, with $\beta = 1$ corresponding to the special case of single exponential kinetics. The kinetics become increasingly stretched with decreasing β. Stretched exponential behaviour, which has also been referred to as 'strange' kinetics (91), has recently gained attention both in theoretical (92, 93) and in experimental work on biological systems. The best-studied experimental model is the structural relaxation of myoglobin at low temperature (94) or at high solvent viscosity (95). A prerequisite for strange kinetics is a rough energy landscape with significant barriers between a large number of local minima (92). Thus, it was argued that protein-folding reactions might exhibit stretched behaviour, under conditions where local minima on the folding landscape become stabilized (e.g. at low temperature). Up to now there has been only one experimental report on strange kinetics in protein folding, which describes the refolding of ubiquitin and phosphoglycerate kinase at low temperature on the μs timescale (96). The difficulty of unambiguously assigning the observed kinetics to stretched behaviour may be seen from the fact that the kinetics only cover about 2.5 magnitudes of lifetimes and can also be described by the sum of two or three exponentials. Nevertheless, these first indications of non-exponential behaviour in protein folding on the very

fast timescale provide an interesting new aspect to the understanding of the energy landscapes for protein folding (see Chapter 5 for further discussion of non-exponential kinetics).

7. Theories of reaction rates

Transition landscapes for protein folding are often complex and may involve sequential and parallel barrier-crossing events, even in the absence of populated intermediates. In addition, folding occurs in an aqueous environment, which contributes significantly to the folding process, as seen in the temperature dependence of protein stability and folding rates. For these scenarios, transition-state theory will not be useful in the quantitative analysis of kinetic data. In the following sections we shall discuss briefly some basic theories relating the rate constant of a reaction to an energy barrier, in order to find a theory more appropriate for protein-folding reactions.

7.1 The van't Hoff–Arrhenius equation

In 1884 van't Hoff published a pioneering textbook on chemical dynamics (97) in which he discussed the temperature dependence of chemical equilibria. In this work he proposed several possible equations to describe the temperature dependence of rate constants. Based on these considerations, Arrhenius argued in 1889 (98) that expressing the rate constant as a function of inverse temperature β ($\beta^{-1} = k_B T$) on a logarithmic scale is physically most meaningful and in accordance with experimental results. In this treatment the rate of escape, k, from a metastable state in a chemical reaction is the product of a temperature-independent pre-exponential factor A and an exponential contribution, which depends on inverse temperature and on the activation energy, E_a:

$$k = A \cdot \exp(-\beta \cdot E_a). \qquad [25]$$

This equation explained the commonly observed strong temperature dependence of chemical reactions, which could not be accounted for solely by an increase in molecular translational energies. Although experimental data were often better described by using a temperature-dependent pre-exponential factor (99), the van't Hoff–Arrhenius equation (eqn 25) was generally considered to be best suited to relate a rate constant to an energy barrier. However, the formulation of a satisfactory treatment of the pre-exponential factor, A, caused considerable difficulty and hampered the molecular interpretation of the van't Hoff–Arrhenius equation. It took more than 40 years before Eyring (24, 100) and, independently, Evans and Polanyi (101, 102) in 1935 developed a simple and general formulation of how small molecules escape from a metastable state (the transition-state theory). This work was based on the pioneering contributions to fluctuation theories by Lord Rayleigh (103), Einstein (104, 105), von Smoluchowski (106–109), Fokker (110), Planck (111), Ornstein (112), and many others.

7.2 Conventional transition-state theory

Transition-state theory assumes that the state with the highest energy (the transition state or activated state) can be treated as a distinct and well-defined state in equilibrium with the reactant, with a quasi-equilibrium constant, $K^{\ddagger}$ (24). The rate of escape, k, thus depends on the Gibbs free energy of activation, $\Delta G^{\circ\ddagger}$, and on a pre-exponential factor reflecting the maximum rate for the reaction in the absence of free-energy barriers:

$$k = \frac{\kappa \cdot k_B T}{h} \cdot e^{-\beta \cdot \Delta G^{\circ\ddagger}} \equiv \kappa \cdot k_{CTST}. \qquad [26]$$

The parameter κ was originally introduced by Eyring as an *ad hoc* fudge factor or transmission coefficient which corrects for those reactive particles that re-cross the transition state (24). Clearly this fact always reduces the reaction rate and therefore $\kappa \leq 1$. Setting $\kappa \equiv 1$ results in what is commonly known as the conventional transition-state theory (CTST). Comparison of transition-state theory with the van't Hoff–Arrhenius equation and using the relationship $\Delta G^{\circ\ddagger} = \Delta H^{\circ\ddagger} - T\Delta S^{\circ\ddagger}$ shows that the pre-exponential factor (A) in the Arrhenius equation corresponds to $\kappa \cdot k_B T/h \cdot e^{[(\Delta S^{\circ\ddagger}+R)/R]}$ and that $E_a = \Delta H^{\circ\ddagger} + RT$.

CTST was initially developed for gas-phase reactions (24) and only later extended to reactions in solution (100). It describes the escape rate of locally trapped small molecules over a potential barrier along a simple linear reaction coordinate. All the reactions considered involve making and breaking covalent bonds and the pre-exponential factor was therefore assumed to correspond to the vibrational motion of a chemical bond, which is of the order of $6 \times 10^{12}\,s^{-1}$ at room temperature. Considering the complexity of protein-folding reactions, which involve motion of the polypeptide chain in solution and simultaneous making and breaking of many non-covalent intra- and intermolecular interactions, it is immediately obvious that TST is not adequate for their treatment. For these reasons, a reaction-rate theory based on diffusional motions in aqueous solvents should be better suited to describe protein folding.

7.3 Kramers' theory

In 1940 Kramers published a famous paper entitled 'Brownian motion in a field of force and the diffusion model of chemical reactions' (113). He considered a particle trapped in a one-dimensional potential well separated by a barrier from a second, deeper well. Kramers' problem was to find the rate of escape of the particle from the well over the barrier. He envisaged the escape process of the particle immersed in a medium as the consequence of Brownian motion driven by thermal forces. The medium exerts a friction on the particle but the thermal forces can, in turn, activate the particle via the fluctuation–dissipation theorem to gain enough energy to escape from the well. The motion of the particle is described by the Langevin equation:

$$m\frac{d^2x}{dt^2} + \gamma\frac{dx}{dt} + \frac{dV}{dx} = F_{ext}(t) \qquad [27]$$

where m denotes the particle mass; $x(t)$, the coordinate; $V(x)$, the potential energy surface of the particle; γ, the friction coefficient; and $F_{ext}(t)$ represents the external thermal excitation from the bath (solvent).

Kramers observed three different regions for the effect of viscosity on the rate of a barrier-crossing event. In the low-friction limit, the rate actually increases with increasing friction, since the system is only weakly coupled to the medium and an equilibrium distribution of reactants cannot be maintained. In other words, the medium cannot efficiently activate the reaction because there are too few interactions with the reactants. With increasing viscosity, friction eventually becomes high enough to maintain an equilibrium distribution of energized reactants, but not yet to perturb the barrier-crossing event. Under these conditions (the intermediate friction limit) the rate of the reaction is independent of solvent friction and the results from Kramers' theory and from CTST approach each other. At even higher friction, which is applicable to reactions in solution, the rate of a reaction decreases with solvent friction, due to barrier re-crossing events before the products are formed (the high friction limit). Kramers demonstrated that, in the high friction limit, transition-state theory seriously overestimates the true rate of escape in most cases. He showed, by solving the Smoluchowski diffusion equation, that the solution for the rate of escape in the high friction limit is simply

$$k \propto \frac{1}{\gamma} \cdot \exp(-\beta \cdot \Delta G^{\circ\ddagger}). \qquad [28]$$

Thus, Kramers' theory predicts a viscosity dependence of the rate constants for reactions in solution. It has been applied successfully to the description of a large number of dynamic processes since it was first formulated. Extensions of Kramers' theory and its application to the treatment of various systems are described in a excellent review by Hänngi *et al.* (114). Since Kramers' theory makes no *ad hoc* assumptions as to the nature of the barrier-crossing events and regards diffusive events as elementary steps in a dynamic process, it should be well suited for the treatment of protein-folding reactions (115). This is supported by the strong viscosity dependence of folding reactions observed experimentally for several proteins (116–118).

8. Application of Kramers' theory to protein folding

Following Kramers' theory, the escape rates for two-state folding, k_u and k_f, are given by the expressions

$$k_u = \nu_u \cdot \exp(-\beta \cdot \Delta G_u^{\circ\ddagger})$$

and

$$k_f = \nu_f \cdot \exp(-\beta \cdot \Delta G_f^{\circ\ddagger}), \qquad [29]$$

where ν_u and ν_f are the Kramers pre-exponential factors for the unfolding and refolding reactions, respectively. In the high friction limit the pre-exponential factors are inversely proportional to the solvent viscosity, η. The dynamics in native and unfolded proteins are influenced by the friction imposed by the solvent and by an

internal friction, e.g. chain stiffness or hindered motions in native or partially folded states. Assuming that these contributions to overall friction are additive, the pre-exponential factors, ν, can be written in the following form (119):

$$\nu_u = \frac{C_u}{(\eta_{solvent} + \sigma_N)} \qquad [30]$$

$$\nu_f = \frac{C_f}{(\eta_{solvent} + \sigma_U)}$$

where C_u and C_f are constants which depend on the potential energy surface, η is the solvent viscosity, and σ is the internal viscosity arising from internal friction. Since the equilibrium of a reaction is always determined by the escape rates for folding and unfolding (eqn 6) the free energy for folding, $\Delta G°$, becomes

$$\begin{aligned}\Delta G° = -\beta^{-1} \cdot \ln\left(\frac{k_f}{k_u}\right) &= -\beta^{-1} \cdot \ln\left[\frac{\nu_f}{\nu_u} \cdot \exp\{-\beta(\Delta G_f^{\circ\ddagger} - \Delta G_u^{\circ\ddagger})\}\right] \\ &= -\beta^{-1} \cdot \ln[\exp\{-\beta(\Delta G_f^{\circ\ddagger} + \beta^{-1} \cdot \ln(\nu_u/\nu_f) - \Delta G_u^{\circ\ddagger})\}] \\ &= \Delta G_f^{\circ\ddagger} + \Delta G_\nu^\circ - \Delta G_u^{\circ\ddagger} \qquad [31]\end{aligned}$$

where we defined a free energy contribution from the pre-exponential factors as

$$\Delta G_\nu^\circ \equiv \beta^{-1} \cdot \ln(\nu_u/\nu_f). \qquad [32]$$

As a consequence of eqn 32, $\Delta G°$ does generally not reflect the difference in the free-energy barriers for folding and unfolding, $\Delta G_f^{\circ\ddagger}$ and $\Delta G_u^{\circ\ddagger}$ respectively (Fig. 8). There is an inherent contribution from the pre-exponential factors which cannot be determined by equilibrium methods. Equation 31 simplifies, however, if the pre-exponential factors for the forward and the backward reaction are identical and ΔG_ν° becomes zero. If we assume the constants C_u and C_f to be equal, we can easily derive an upper limit for the contribution of ΔG_ν° to protein stability:

$$\Delta G_\nu^\circ = \beta^{-1} \cdot \ln\left(\frac{\eta_{solvent} + \sigma_U}{\eta_{solvent} + \sigma_N}\right) \geq \beta^{-1} \cdot \ln\left(\frac{1}{1 + \sigma_N}\right) = -\beta^{-1} \cdot \ln(1 + \sigma_N). \qquad [33]$$

Folding starts from a solvated polypeptide chain in water with little internal friction compared to solvent friction (120) and thus we neglect σ_U for the refolding reaction. For the unfolding reaction, starting from native protein, the internal viscosity σ_N will be significant due to the restricted motion of the polypeptide chain. For sperm whale myoglobin, the internal viscosity, σ, at room temperature was measured to be 4.1 ± 1.3 cP (119). This gives an estimate of the pre-exponential contribution to the overall stability of sperm whale myoglobin of approximately –1 kcal/mol. These considerations show that in the case of myoglobin the difference in the pre-exponential factors for unfolding and refolding will contribute maximally 1 kcal/mol to the equilibrium stability of the native protein. The free-energy barrier for unfolding is overestimated by the same amount when transition-state theory is

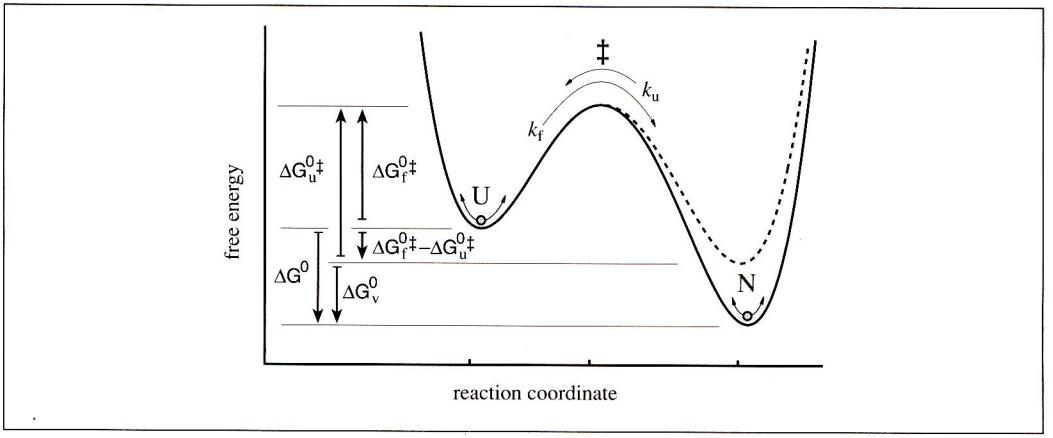

Fig. 8. Effects of different pre-exponential factors for the refolding and unfolding reactions on the free-energy changes in a two-state folding reaction (cf. eqns 29–33). The dashed line represents the free-energy profile assuming identical pre-exponential factors for the folding and unfolding reaction. The solid lines assumes differences in the pre-exponential factors, resulting in an additional contribution, ΔG_v° to the free energy of folding, ΔG°.

applied. This value represents an upper limit, since the internal friction increases along the reaction coordinate of the folding process and the effective internal friction for refolding might be higher. However, the strong viscosity dependence of the folding reaction of several two-state proteins suggests that solvent viscosity indeed dominates over internal viscosity (117, 118). Due to the lack of data for the internal viscosity in folded states of other proteins, the magnitude of the contribution may vary slightly.

In general, we cannot expect the pre-exponential factors for the unfolding rate ν_u and for the folding rate ν_f to be independent of the solvent conditions such as denaturant concentration [D], temperature, and pressure. This will contribute to the experimentally determined m-values and the activation parameters ($\Delta H^{\circ‡}$, $\Delta S^{\circ‡}$, $\Delta V^{\circ‡}$, and $\Delta V_p^‡$.

9. The pre-exponential factor for protein-folding reactions

An adequate pre-exponential factor for protein folding should contain contributions from solvent and internal friction. However, these considerations are not able to give absolute values for the pre-exponential factors, which are crucial for the determination of the absolute scale of the free-energy barriers. A realistic estimate for a pre-exponential factor must consider the elementary steps of a protein-folding reaction, which should be closely related to the motions of the polypeptide chain. During folding the polypeptide chain searches the conformational space for energetically favourable states by making contacts between different parts of the chain. In this

scenario intrachain diffusion can be regarded as the elementary process in protein folding. Free diffusion in solutions was treated extensively almost 100 years ago (106, 121, 122) but until recently, little was known about the absolute rates of diffusion restricted by chain motions in polypeptides. Numerous theoretical studies have been made to investigate the process of intrachain diffusion in polymers (17, 123–126). Using a first passage time approach, Szabo *et al.* (124) predicted single exponential behaviour for intrachain contact formation, when the interconversion between individual conformations is fast and when the relative number of conformations allowing end-to-end contact is small. (This is similar to Zwanzig's results discussed above on barrier-free protein folding via escape states (88).) These studies were not able to give absolute numbers, but they predicted that the rate of contact formation scales with $N^{-1.5}$ for intrachain diffusion processes in polymers, where N is the number of polymer building blocks, viz. the number of amino acids in the case of a polypeptide chain. This value is in agreement with the earlier treatment of a similar process by Jacobsen and Stockmayer (123).

Early experimental work on polypeptide chain dynamics was aimed at determining average diffusion constants for polypeptide motion. Haas and co-workers studied chain dynamics using resonance-energy transfer (singlet energy transfer) between donor and acceptor groups attached at the ends of short peptides (127). These experiments are sensitive for relative motions between the donor and the acceptor at distances near the characteristic transfer distance (R_0) for a given donor/acceptor pair—22 Å for the chosen system. The resulting diffusion constants were in the range of 2.6×10^7 to $6.4 \times 10^7\,cm^2\,s^{-1}$ for donor–acceptor separations between 5 and 9 peptide bonds, which converts into time constants between 9 and 3 ns for contact formation at van der Waals distance. Since resonance-energy transfer should be sensitive for a broad spectrum of motions near R_0, it is not clear whether these results can be applied directly to contact formation. They still, however, give a very good estimate for the timescales of peptide motion.

Photochemical triggering and nanosecond-resolved optical spectroscopy were used by Eaton and co-workers to measure intrachain diffusion directly in reduced cytochrome *c* at high concentrations of denaturant (128, 129). They obtained a time constant of about 40 μs for haem binding to methionine residues located 50–60 residues further along the polypeptide chain. Since extrinsic methionine binds to haem in a nearly diffusion-controlled process, the 40 μs reaction was proposed to reflect the rate of intrachain diffusion between the two chain segments. Use of the scaling law given by Szabo *et al.* (124) allowed extrapolation of this rate to shorter distances, yielding an estimate of 1 μs for the time constant of contact formation at a distance of 10 peptide bonds. This is thought to be the distance at which contact formation is fastest, due to increasing chain stiffness in shorter chain segments (18, 130, 131). Since the system is not completely diffusion controlled and contact formation between an amino acid and the very large haem group was being monitored, it is not clear whether these rate constants reflect the process of intrachain diffusion.

The first direct experimental data on maximum rates of intrachain diffusion

between different parts of a polypeptide chain were obtained by Bieri *et al.* (120) using triplet–triplet energy transfer. Energy transfer between an excited triplet donor and an acceptor proceeds by a two-electron transfer mechanism (Dexter mechanism), which requires van der Waals contact between the two groups (132). A series of short, unstructured peptides were synthesized in which the distance between a triplet donor and a triplet acceptor was varied by insertion of 1 to 4 glycine–serine pairs. Due to the special properties of glycine, these peptides are particularly flexible and exhibit short end-to-end distances (133), making them good model systems for evaluating the maximum rate of intrachain diffusion. The results show that contact formation fits well to single-exponential kinetics and the rate increases with decreasing chain length (N), even for the shortest peptides. The rates decrease with an $N^{-1.3 \pm 0.2}$ dependence in this limited region, which is well within the range of the predicted values of $k \sim N^{-1.5}$ (123, 124). Intrachain contact formation in the peptide models is strongly viscosity dependent, showing that solvent friction is the limiting factor (120). The maximum rate of contact formation was 10–20 ns at a viscosity of 1 cP for the shortest peptides, in which donor and acceptor are separated by three peptide bonds. This should represent the upper limit at which local structural elements can form and allows an estimate of the height of the free-energy barrier for protein-folding reactions. These rates are only slightly smaller for less-flexible peptides, which do not contain Gly residues (Bieri *et al.*, unpublished).

Using these values for the pre-exponential factor in eqn 29, we can calculate the height of the free-energy barrier for experimentally determined folding reactions. The fastest experimentally determined folding reactions are of the order of 10^3–$10^4\,s^{-1}$. Assuming a pre-exponential factor of $10^8\,s^{-1}$ gives $\Delta G^{\circ\ddagger}$ of 5–6 kcal/mol at room temperature, which corresponds to 9–11 k_BT. For comparison, using CTST, the same rate constants will result in $\Delta G^{\circ\ddagger}$ of 12–14 kcal/mol or 20–22 k_BT.

The pre-exponential factor for the unfolding reaction will be strongly correlated with the motions of the polypeptide chain in the native state, which have been shown to contain significant contributions from internal viscosity (σ) (119). Using the maximum rate of chain motion in the unfolded state and its viscosity dependence (120), in combination with experimentally determined σ_N values for native proteins, we can calculate the pre-exponential factor for unfolding using eqn 30. The σ_N value of 4.1 cP measured for native myoglobin results in a pre-exponential factor of about $2 \times 10^7\,s^{-1}$ for the unfolding process. Since the mechanism of unfolding is not well understood, there might be significant contributions to the barrier-crossing events from other processes, like the entry of water into the hydrophobic core.

10. Conclusions and outlook

A quantitative treatment of folding kinetics is a prerequisite for elucidating mechanisms of protein folding. Even simple kinetics, like single exponential behaviour, can be caused by a variety of different folding landscapes. Therefore the interplay between theoretical models and experimental results is essential in the effort to understand protein folding. We have seen that concepts from classical reaction-rate

theory developed for simple chemical reactions can be applied to protein folding, since the energy landscapes for most proteins seem to contain partially folded intermediates, even if they do not become populated. However, it is also obvious that results obtained using transition-state theory have to be treated with caution. A much better model for analysing protein-folding reactions is provided by Kramers' theory. The aim of future experimental work will be to gain a better understanding of the very early steps of folding reactions and of the complexity of the transition barriers separating native from unfolded proteins.

References

References marked * are recommended for further reading.

1. Levinthal, C. (1969) How to fold graciously. In *Mössbauer spectroscopy in biological systems*, DeGrunner, P., Tsigris, J. C. M., and Münck, E. (eds.). Monticello, Illinois, p. 22.
2. Tanford, C. (1968) Protein denaturation. Part A. Characterization of the denatured state. *Adv. Prot. Chem.*, **23**, 121.
3. Tanford, C. (1968) Protein denaturation. Part B. The transition from native to denatured state. *Adv. Prot. Chem.*, **23**, 218.
4. Tanford, C. (1970) Protein denaturation. Part C. Theoretical models for the mechanism of denaturation. *Adv. Prot. Chem.*, **24**, 1.
5. Baldwin, R. L. (1975) Intermediates in protein folding reactions and the mechanism of protein folding. *Annu. Rev. Biochem.*, **44**, 453.
6. Kim, P. S. and Baldwin, R. L. (1982) Specific intermediates in the folding reactions of small proteins and the mechanism of protein folding. *Annu. Rev. BioChem.*, **51**, 459.
7. Kim, P. S. and Baldwin, R. L. (1990) Intermediates in the folding reactions of small proteins. *Annu. Rev. Biochem.*, **59**, (631), 631.
8. Jaenicke, R. (1987) Folding and association of proteins. *Progr. Biophys. Mol. Biol.*, **49**, 117.
9. Schmid, F. X. (1992) The mechanism of protein folding. *Curr. Opin. Struct. Biol.*, **2**, 21.
10. Jaenicke, R. (1999) Stability and folding of domain proteins. *Progr. Biophys. Mol. Biol.*, **71**, 155.
11. Zwanzig, R., Szabo, A., and Bagchi, B. (1992) Levinthal's paradox. *Proc. Natl. Acad. Sci., USA*, **89**, 20.
12. Bryngelson, J. D. and Wolynes, P. G. (1987) Spin glasses and the statistical mechanics of protein folding. *Proc. Natl. Acad. Sci., USA*, **84**, 7524.
13. Bryngelson, J. D. and Wolynes, P. G. (1989) Intermediates and barrier crossing in a random model (with applications to protein folding). *J. Phys. Chem.*, **93**, 6902.
14. Bryngelson, J. D., Onuchic, J. N., Socci, N. D., and Wolynes, P. G. (1995) Funnels, pathways, and the energy landscape of protein folding: A synthesis. *Proteins: Struct. Funct. Genet.*, **21**, 167.
*15. Wolynes, P. G., Onuchic, J. N., and Thirumalai, D. (1995) Navigating the folding routes. *Science*, **267**, 1619.
16. Thirumalai, D. (1994) Theoretical perspectives on in vitro and in vivo protein folding. In *Statistical mechanics, protein structure, and protein substrate interactions*, Doniach, S. (ed.). Plenum Press, pp. 115–134.
17. Thirumalai, D. (1995) From minimal models to real protein: time scales for protein folding kinetics. *J. Phys.*, **5**, 1457.

18. Guo, Z. and Thirumalai, D. (1995) Kinetics of protein folding: nucleation mechanism, time scales, and pathways. *Biopolymers*, **36**, 83.
19. Chan, H. S. and Dill, K. A. (1994) Transition states and folding dynamics of proteins and heteropolymers. *J. Chem. Physics*, **100**, 9238.
20. Kiefhaber, T. (1995) Protein folding kinetics. In *Methods in molecular biology*, Vol. 40: *Protein stability and folding protocols*, Shirley, B. A. (ed). Humana Press, Totowa, NJ, p. 313.
*21. Szabo, Z. G. (1969) Kinetic characterization of complex reaction systems. In *Comprehensive chemical kinetics*, Vol. 2, Bamford, C. H. and Tipper, C. F. H. (ed.). Elsevier, Amsterdam, pp. 1–80.
22. Moore, J. W. and Pearson, R. G. (1981) *Kinetics and mechanisms*. John Wiley and Sons, New York.
23. Jackson, S. E. (1998) How do small proteins fold? *Folding and Design*, **3**, R81.
24. Eyring, H. (1935) The activated complex in chemical reactions. *J. Chem. Phys.*, **3**, 107.
25. Aune, K. C. and Tanford, C. (1969) Thermodynamics of the denaturation of lysozyme by guanidine hydrochloride. II Dependence on denaturant concentration at 25 degrees. *Biochemistry*, **11**, 4586.
26. Myers, J. K., Pace, C. N., and Scholtz, J. M. (1995) Denaturant m-values and heat capacity changes: relation to changes in accessible surface areas of protein unfolding. *Protein Sci.* **4**, 2138.
27. Jackson, S. E. and Fersht, A. R. (1991) Folding of chymotrypsin inhibitor 2.1. Evidence for a two-state transition. *Biochemistry*, **30**, 10428.
28. Kuwajima, K., Mitani, M., and Sugai, S. (1989) Characterization of the critical state in protein folding. Effects of guanidine hydrochloride and specific Ca^{2+} binding on the folding kinetics of alpha-lactalbumin. *J. Mol. Biol.*, **206**, 547.
29. Pohl, F. M. (1976) Temperature-dependence of the kinetics of folding of chymotrysinogen A. *FEBS Lett.*, **65**, 293.
30. Oliveberg, M., Tan, Y.-J., and Fersht, A. R. (1995) Negative activation enthalpies in the kinetics of protein folding. *Proc. Natl Acad. Sci., USA*, **92**, 8926.
31. Schindler, T. and Schmid, F. X. (1996) Thermodynamic characterization of an extremely rapid protein folding reaction. *Biochemistry*, **51**, 16833.
32. Schönbrunner, N., Koller, K.-P., and Kiefhaber, T. (1997) Folding of the disulfide-bonded β-sheet protein tendamistat: Rapid two-state folding without hydrophobic collapse. *J. Mol. Biol.*, **268**, 526.
33. Scalley, M. L. and Baker, D. (1997) Protein folding kinetics exhibit an Arrhenius temperature dependence when corrected for the temperature dependence of protein stability. *Proc. Natl Acad. Sci., USA*, **94**, 10636.
34. Baldwin, R. L. (1986) Temperature dependence of the hydrophobic interaction in protein folding. *Proc. Natl Acad. Sci., USA*, **83**, (21), 8069.
35. Baldwin, R. L. and Muller, N. (1992) Relation between the convergence temperatures Th* and Ts* in protein unfolding. *Proc. Natl Acad. Sci., USA*, **89**, 7110.
36. Heremans, K. (1982) High pressure effects on proteins and other biomolecules. *Ann. Rev. Biophys. Bioeng.*, **11**, 1.
37. Dill, K. A. (1990) Dominant forces in protein folding. *Biochemistry*, **29**, 7133.
38. Hummer, G., Garde, S., Garcia, A. E., Paulaitis, M. E., and Pratt, L. R. (1998) The pressure dependence of hydrophobic interactions is consistent with the observed pressure denaturation of proteins. *Proc. Natl Acad. Sci., USA*, **95**, 1552.
39. Klapper, M. H. (1971) On the nature of the protein interior. *Biochim. Biophys. Acta*, **229**, 557.

40. Gerstein, M. and Chothia, C. (1996) Packing at the protein–water interface. *Proc. Natl Acad. Sci., USA*, **93**, 10167.
41. Frye, K. J. and Royer, C. A. (1998) Probing the contribution of internal cavities to the volume change of protein unfolding under pressure. *Protein Sci.*, **7**, 2217.
42. Planck, M. (1887) Ueber das Princip der Vermehrung der Entropie. *Ann. Phys. Chem.*, **32**, 462.
43. Vidugiris, G. J. A., Markley, J. L., and Royer, C. A. (1995) Evidence for a molten globule-like transition state in protein folding from determination of activation volumes. *Biochemistry*, **34**, 4909.
44. Jacob, M., Holtermann, G., Perl, D., Reinstein, J., Schindler, T., Geeves, M., and Schmid, F. X. (1999) Microsecond folding of the cold-shock protein measured by a pressure-jump technique. *Biochemistry*, **38**, 2882.
45. Pappenberger, G., Saudan, C., Becker, M., Merbach, A. E., and Kiefhaber, T. (2000) Denaturant-induced movement of the transition state of protein folding revealed by high pressure stopped-flow measurements. *Proc. Natl. Acad. Sci., USA*, **97**, 17.
46. Ikai, A. and Tanford, C. (1973) Kinetics of unfolding and refolding of proteins. I. Mathematical Analysis. *J. Mol. Biol.*, **73**, 145.
47. Kiefhaber, T., Kohler, H. H., and Schmid, F. X. (1992) Kinetic coupling between protein folding and prolyl isomerization. I. Theoretical models. *J. Mol. Biol.*, **224**, 217.
48. Garel, J. R. and Baldwin, R. L. (1973) Both the fast and slow folding reactions of ribonuclease A yield native enzyme. *Proc. Natl. Acad. Sci., USA*, **70**, 3347.
49. Brandts, J. F., Halvorson, H. R., and Brennan, M. (1975) Consideration of the possibility that the slow step in protein denaturation reactions is due to *cis–trans* isomerism of proline residues. *Biochemistry*, **14**, 4953.
50. Kiefhaber, T., Grunert, H. P., Hahn, U., and Schmid, F. X. (1990) Replacement of a *cis* proline simplifies the mechanism of ribonuclease T1 folding. *Biochemistry*, **29**, 6475.
51. Schultz, D. A., Schmid, F. X., and Baldwin, R. L. (1992) *Cis* proline mutants of ribonuclease A. 2. Elimination of the slow-folding forms by mutation. *Protein Sci.*, **1**, 917.
52. Dodge, R. W. and Scheraga, H. A. (1996) Folding and unfolding kinetics of the proline-to-alanine mutants of bovine pancreatic ribonuclease A. *Biochemistry*, **35**, 1548.
53. Colon, W., Wakem, L. P., Sherman, F., and Roder, H. (1997) Identification of the predominant non-native histidine ligand in unfolded cytochrome c. *Biochemistry*, **36**, 12535.
54. Yeh, S.-R. and Rousseau, D. L. (1998) Folding intermediates in cytochrome c. *Nature Struct. Biol.*, **5**, 222.
55. Yeh, S.-R., Takahashi, S., Fan, B., and Rousseau, D. L. (1998) Ligand exchange in unfolded cytochrome *c* folding. *Nature Struct. Biol.*, **4**, 51.
56. Segel, D., Bachmann, A., Hofrichter, J., Hodgson, K., Doniach, S., and Kiefhaber, T. (1999) Characterization of transient intermediates in lysozyme folding with time-resolved small angle X-ray scattering. *J. Mol. Biol.*, **288**, 489.
57. Wu, L. C., Peng, Z.-Y., and Kim, P. S. (1995) Bipartite structure of the α-lactalbumin molten globule. *Nature Struct. Biol.*, **2**, 281.
58. Wu, L. C. and Kim, P. S. (1998) A specific hydrophobic core in the α-lactalbumin molten globule. *J. Mol. Biol.*, **280**, 175.
59. Luo, Y., Kay, M. S., and Baldwin, R. L. (1997) Cooperativity of folding of the apomyoglobin pH 4 intermediate studied by glycine and proline mutations. *Nature Struct. Biol.*, **4**, 925.
60. Hill, T. L. (1974) The sliding filament model of contraction of striated muscle. *Progr. Biophys. Mol. Biol.*, **28**, 267.

61. Hill, T. L. (1977) *Free energy transduction in biology*. Academic Press, London.
62. Weismann, J. S. and Kim, P. S. (1991) Re-examination of the folding of BPTI: predominance of native intermediates. *Science*, **253**, 1386.
63. Kiefhaber, T., Grunert, H. P., Hahn, U., and Schmid, F. X. (1992) Folding of RNase T1 is decelerated by a specific tertiary contact in a folding intermediate. *Proteins: Struct. Funct. Genet.*, **12**, 171.
64. Silow, M. and Oliveberg, M. (1997) Transient intermediates in protein folding are easily mistaken for folding intermediates. *Proc. Natl. Acad. Sci., USA*, **94**, 6084.
65. Blake, C. C. F., Koenig, D. F., Mair, G. A., North, A. C. T., Phillips, D. C., and Sarma, V. F. (1967) Structure of hen egg-white lysozyme. *Nature*, **206**, 757.
66. Blake, C. C. F., Mair, G. A., North, A. C. T., Phillips, D. C., and Sarma, V. F. (1967) On the conformation of the hen egg-white lysozyme molecule. *Proc. Roy. Soc. B*, **167**, 365.
67. Kuwajima, K., Hiraoka, Y., Ikeguchui, M., and Sugai, S. (1985) Comparison of the transient folding intermediates in lysozyme and α-lactalbumin. *Biochemistry*, **24**, 874.
68. Chaffotte, A. F., Guillou, Y., and Goldberg, M. E. (1992) Kinetic resolution of peptide bond and side-chain far-UV CD during folding of HEWL. *Biochemistry*, **31**, 9694.
69. Radford, S. E., Dobson, C. M., and Evans, P. A. (1992) The folding of hen lysozyme involves partially structured intermediates and multiple pathways. *Nature*, **358**, 302.
70. Itzhaki, L. S., Evans, P. A., Dobson, C. M., and Radford, S. E. (1994) Tertiary interactions in the folding pathway of hen lysozyme: kinetic studies using fluorescent probes. *Biochemistry*, **33**, 5212.
71. Kiefhaber, T. (1995) Kinetic traps in lysozyme folding. *Proc. Natl. Acad. Sci., USA*, **92**, 9029.
*72. Schmid, F. X. (1983) Mechanism of folding of ribonuclease A. Slow refolding is a sequential reaction via structural intermediates. *Biochemistry*, **22**, 4690.
*73. Wildegger, G. and Kiefhaber, T. (1997) Three-state model for lysozyme folding: triangular folding mechanism with an energetically trapped intermediate. *J. Mol. Biol.*, **271**, 294.
74. Bieri, O., Wildegger, G., Bachmann, A., Wagner, C., and Kiefhaber, T. (1999) A salt-induced intermediate is on a new parallel pathway of lysozyme folding. *Biochemistry*, **38**, 12460.
75. Ikai, A., Fish, W. W., and Tanford, C. (1973) Kinetics of unfolding and refolding of proteins. II. Results for cytochrome *c*. *J. Mol. Biol.*, **73**, 165.
76. Jonsson, T., Waldburger, C. D., and Sauer, R. T. (1996) Nonlinear free energy relationship in arc repressor unfolding imply the existence of unstable, native-like folding intermediates. *Biochemistry*, **35**, 4795.
77. Schönbrunner, N., Pappenberger, G., Scharf, M., Engels, J., and Kiefhaber, T. (1997) Effect of pre-formed correct tertiary interactions on rapid two-state tendamistat folding: evidence for hairpins as initiation sites for β-sheet formation. *Biochemistry*, **36**, 9057.
78. Kiefhaber, T., Bachmann, A., Wildegger, G., and Wagner, C. (1997) Direct measurements of nucleation and growth rates in lysozyme folding. *Biochemistry*, **36**, 5108.
79. Walkenhorst, W. F., Green, S., and Roder, H. (1997) Kinetic evidence for folding and unfolding intermediates in staphylococcal nuclease. *Biochemistry*, **36**, 5795.
80. Oliveberg, M., Tan, Y.-J., Silow, M., and Fersht, A. R. (1998) The changing nature of the protein folding transition state: implications for the free-energy profile for folding. *J. Mol. Biol.*, **277**, 933.
81. Silow, M. and Oliveberg, M. (1997) High-energy channeling in protein folding. *Biochemistry*, **36**, 7633.
82. Hammond, G. S. (1955) A correlation of reaction rates. *J. Am. Chem. Soc.*, **77**, 334.

83. Matouschek, A., Otzen, D. E., Itzhaki, L., Jackson, S. E., and Fersht, A. R. (1995) Movement of the transition state in protein folding. *Biochemistry*, **34**, 13656.
84. Otzen, D., Kristense, O., Proctor, M., and Oliveberg, M. (1999) Structural changes in the transition state of protein folding: alternative interpretations of curved chevron plots. *Biochemistry*, **38**, 6499.
85. Wolynes, P. G. (1997) Folding funnels and energy landscapes of larger proteins within the capillarity approximation. *Proc. Natl. Acad. Sci., USA*, **94**, 6170.
86. Portman, J. J., Takada, S., and Wolynes, P. G. (1998) Variational theory for site resolved protein folding free energy surfaces. *Phys. Rev. Lett.*, **81**, 5237.
87. Wagner, C. and Kiefhaber, T. (1999) Intermediates can accelerate protein folding. *Proc. Natl. Acad. Sci., USA*, **96**, 6716.
*88. Zwanzig, R. (1997) Two-state models for protein folding. *Proc. Natl Acad. Sci., USA*, **94**, 148.
89. Zhou, H.-X. and Zwanzig, R. (1991) A rate process with an entropic barrier. *J. Chem. Phys.*, **94**, 6147.
90. Kohlrausch, R. (1847) Über das Dellmann'sche Elektrometer. *Ann. der Physik und Chemie*, **11**, 353.
91. Shlesinger, M. F., Zaslavsky, G. M., and Klafter, J. (1993) Strange kinetics. *Nature*, **363**, 31.
92. Saven, J. G., Wang, J., and Wolynes, P. G. (1994) Kinetics of protein folding: The folding dynamics of globally connected rough energy landscapes with biases. *J. Chem. Phys.*, **101**, 11037.
93. Skorobogatiy, M., Guo, H., and Zuckermann, M. (1998) Non-Arrhenius behaviour in the relaxation of model proteins. *J. Chem. Phys.*, **109**, 2528.
94. Austin, R. H., Beeson, K. W., Eisenstein, L., Frauenfelder, H., and Gunsalus, I. C. (1975) Dynamics of ligand binding to myoglobin. *Biochemistry*, **14**, 5355.
95. Hagen, S. J., Hofrichter, J., and Eaton, W. A. (1995) Protein kinetics in a glass at room temperature. *Science*, **269**, 959.
96. Sabelko, J., Ervin, J., and Gruebele, M. (1999) Observation of strange kinetics in protein folding. *Proc. Natl. Acad. Sci., USA*, **96**, 6031.
97. van't Hoff, J. H. (1884) *Etudes de dynamique*. Muller, Amsterdam.
98. Arrhenius, S. (1889). Über die Reaktionsgeschwindigkeit bei der Inversion von Rohrzucker durch Säuren. *Z. Phys. Chem.*, **4**, 226.
99. Bodenstein, M. (1899) Gasreaktionen im chemischen Kinetik. II. Einfluss der Temperatur auf Bildung und Zersetzung von Jodwasserstoff. *Z. Phys. Chem.*, **29**, 295.
100. Wynne-Jones, W. F. K. and Eyring, H. (1935) The absolute rate of reactions in condensed phases. *J. Chem. Phys.*, **3**, 492.
101. Evans, M. G. and Polanyi, M. (1935) Some applications of the transition state method to the calculation of reaction velocities, especially in solution. *Trans. Faraday Soc.*, **31**, 875.
102. Evans, M. G. and Polanyi, M. (1937) On the introduction of thermodynamic variables into reaction kinetics. *Trans. Faraday Soc.*, **33**, 448.
103. Lord Raleigh, R. S. (1891) Dynamical problems of the theory of gases. *Philos. Mag.*, **32**, 424.
104. Einstein, A. (1905) Über die von der molekularkinetischen Theorie der Wärme geforderte Bewegung von in ruhenden Flüssigkeiten suspendierten Teilchen. *Ann. Phys.*, **17**, 549.
105. Einstein, A. (1906) Zur Theorie der Brownschen Bewegung. *Ann. d. Phys.*, **19**, 371.
106. von Smoluchowski, M. (1906) Zur kinetischen Theorie der Brownschen Molekularbewegung und der Suspensionen. *Ann. d. Phys.*, **21**, 756.

107. von Smoluchowski, M. V. (1914) *Bull. Acad. Crasovie Classe des sciences mathematiques et naturelles, Serie A*, 418.
108. von Smoluchowski, M. (1915) Über Brownsche Molekularbewegung unter Einwirkung äußerer Kruafte und deren Zusammenhang mit der verallgemeinerten Diffusionsgleichung. *Ann. Phys. (Leipzig)*, **48**, 1103.
109. von Smoluchowski, M. V. (1917) Versuch einer mathematischen Theorie der Koagulationskinetik kolloider Lösung. *Z. Phys. Chem.*, **92**, 129.
110. Fokker, A. D. (1914) Die mittlere Energie rotierender elektrischer Dipole im Strahlungsfeld. *Ann. Phys. (Leipzig)*, **43**, 810.
111. Planck, M. (1917) *Über einen Satz der statistischen Dynamik und seine Erweiterung in der Quantentheorie. Sitzungsber.* Preuss. Akad. Wiss., p. 324.
112. Ornstein, L. S. (1917) The clustering tendency of the molecules at the critical point. *Versl. Acad. Amst.*, **26**, 1005.
113. Kramers, H. A. (1940) Brownian motion in a field of force and the diffusion model of chemical reactions. *Physica*, **4**, 284.
*114. Hänggi, P., Talkner, P., and Borkovec, M. (1990) Reaction-rate theory: fifty years after Kramers. *Rev. Mod. Phys.*, **62**, 251.
115. Klimov, V. and Thirumalai, D. (1997) Viscosity dependence of the folding rates of proteins. *Phys. Rev. Lett.*, **79**, 317.
116. Chrunyk, B. A. and Matthews, C. R. (1990) Role of diffusion in the folding of the a subunit of tryptophan synthase from *Escherichia coli*. *Biochemistry*, **29**, 2149.
117. Jacob, M., Schindler, T., Balbach, J., and Schmid, F. X. (1997) Diffusion control in an elementary protein folding reaction. *Proc. Natl. Acad. Sci., USA*, **94**, 5622.
118. Plaxco, K. W. and Baker, D. (1998) Limited internal friction in the rate-limiting step of a two-state protein folding reaction. *Proc. Natl. Acad. Sci., USA*, **95**, 13591.
119. Ansari, A., Jones, C. M., Henry, E., Hofrichter, J., and Eaton, W. A. (1992) The role of solvent viscosity in the dynamics of protein conformational changes. *Science*, **256**, 1796.
120. Bieri, O., Wirz, J., Hellrung, B., Schutkowski, M., Drewello, M., and Kiefhaber, T. (1999) The speed limit for protein folding measured by triplet–triplet energy transfer. *Proc. Natl. Acad. Sci., USA*, **96**, 9597.
121. Einstein, A. (1906) Eine neue Bestimmung der Moleküldimensionen. *Ann. d. Phys.*, **19**, 289.
122. von Smoluchowski, M. (1916) Drei Vorträge über Diffusion, Brownsche Molekularbewegung und Koagulation von Kolloidteilchen. *Phys. Z.*, **17**, 557.
123. Jacobsen, H. and Stockmayer, W. H. (1950) Intramolecular reaction in polycondensations. I. The theory of linear systems. *J. Phys. Chem.*, **18**, 1600.
124. Szabo, A., Schulten, K., and Schulten, Z. (1985) First passage time approach to diffusion controlled reactions. *J. Chem., Phys.*, **72**, 4350.
125. de Gennes, P. G. (1985) Kinetics of collapse for a flexible coil. *J. Phys. Lett.*, **46**, L639–L642.
126. Fixman, M. (1987) Brownian dynamics of chain polymers. *Faraday Discuss. Chem. Soc.*, **83**, 199.
127. Haas, E., Katchalski-Katzir, E., and Steinberg, I. Z. (1978) Brownian motion at the ends of oligopeptide chains as estimated by energy transfer between chain ends. *Biopolymers*, **17**, 11.
128. Jones, C. M., Henry, E. R., Hu, Y., Chan, C.-K., Luck, S. D., Byuhan, A., Roder, H., Hofrichter, J., and Eaton, W. A. (1993) Fast events in protein folding initiated by nanosecond laser photolysis. *Proc. Natl. Acad. Sci., USA*, **90**, 11860.

129. Hagen, S. J., Hofrichter, J., Szabo, A., and Eaton, W. A. (1996) Diffusion-limited contact formation in unfolded cytochrome c: Estimating the maximum rate of protein folding. *Proc. Natl. Acad. Sci., USA*, **93**, 11615.
130. Camacho, C. J. and Thirumalai, D. (1995) Theoretical predictions of folding pathways by using the proximity rule, with applications to bovine pancreatic inhibitor. *Proc. Natl. Acad. Sci., USA*, **92**, 1277.
131. Damaschun, G., Damaschun, H., Gast, K., and Zirwer, D. (1998) Denatured states of yeast phosphoglycerate kinase. *Biochemistry, (Moscow)*, **63**, 259.
132. Balzani, V., Bolletta, F., and Scandola, F. (1980) Vertical and 'nonvertical' energy transfer processes. A general classical treatment. *J. Am. Chem. Soc.*, **102**, 2152.
133. Miller, W. G., Brant, D. A., and Flory, P. J. (1967) Random coil configurations of polypeptide chains. *J. Mol. Biol.*, **23**, 67.